Beamforming Analysis of Linear and Planar Arrays for Next-Generation Wireless Systems

Wêndria C. da Silva, João C. Weyl A. Costa, André M. Cavalcante and Karlo Q. da Costa

***Abstract*— This paper presents a detailed analysis of linear and planar dipole antenna arrays with emphasis on near-field beamforming for high-frequency communication, particularly at 28 GHz, a band expected to be relevant for 6G. Using the Method of Moments (MoM), we investigate the impact of array geometry and size on spatial field confinement and multi-user beam steering. Our results demonstrate that planar arrays offer superior spatial resolution, enabling precise control over beam direction and user targeting in dense wireless scenarios. This highlights the potential of ELAA structures for future 6G systems, especially in near-field communication environments.**

Keywords*— *Linear array of dipoles, 6G technology in the near field, Method of Moments.

I. INTRODUCTION

Fifth generation (5G) wireless networks have driven major technological advancements, with an estimated economic impact of up to US$13.2 trillion by 2035 [1]. As a result, there is growing interest in the development of sixth generation (6G) systems, which are expected to meet even stricter performance requirements, including extremely high data rates, ultra-low latency, and massive device connectivity [2]. To achieve such goals, emerging technologies such as reconfigurable intelligent surfaces (RIS), massive multiple-input multiple output (MIMO), and the use of mmWave and Terahertz (THz) bands demand a substantial increase in the number of active elements and operation at higher carrier frequencies, which considerably extends the Rayleigh distance [3].

In this context, Extremely Large Aperture Arrays (ELAAs) have become essential components in 6G systems, supporting operation in the radiating near-field region (Fresnel zone), where electromagnetic wavefronts exhibit spherical curvature, contrasting with the planar approximation adopted in far-field models. Fig. 1 illustrates this transition between the near- and far-field regions [3]-[4]. This shift introduces new spatial Degrees of Freedom (DoF), enabling enhanced beamforming capabilities and improved spectral efficiency, particularly in line-of-sight (LoS) scenarios [3].

In this context, this work presents a detailed study of two dipole antenna arrays—a uniform linear array (ULA) and a uniform planar array (UPA)—operating in the radiative near-field region at 28 GHz. Unlike conventional studies that consider the far field, the analysis presented here emphasizes the effects of near-field propagation on beam focusing, spatial resolution, and separation between multiple users. The influence of array geometry and the number of elements on the electromagnetic field behavior is evaluated, also addressing the trade-offs between performance and computational cost in realistic implementations for next-generation wireless systems.

The use of half-wave dipole elements is motivated by their simplicity, analytical tractability, and well-known radiation characteristics, which make them a common reference model in antenna theory and array studies [5]. Dipoles offer a good balance between performance and implementation feasibility, allowing the effects of geometry and phase control on near-field beamforming to be isolated and clearly analyzed. Furthermore, their linear polarization and predictable input impedance simplify both modeling and fabrication in experimental prototypes.

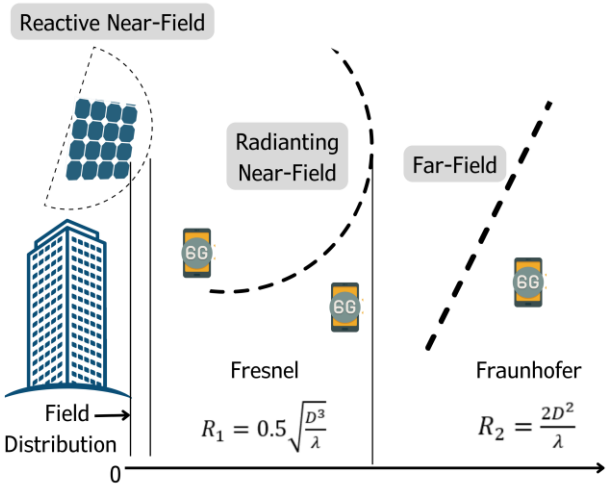

Fig. 1. EM field boundaries and typical changes in the antenna's wavefront shape from the radiating near-field to far-field region.

II. THEORICAL DEVELOPMENT

A. Near-Field Array Description

This section presents the radiation optimization of dipole arrays in the near-field, emphasizing beamforming, a key technique for 6G applications [5]. The approach relies on adjusting the excitation phase of each dipole to focus the beam at a user-defined location near the array, as shown in Fig. 2.

Each dipole is fed by a voltage source modeled as $Vs(m,n) = 1e^{j\phi_{m,n}}$, in which $\phi_{m,n}$ is derived from the path length difference relative to a reference dipole element, ensuring constructive interference at the desired point:

$$\phi_{m,n} = -k \times \Delta_{m,n} \tag{1}$$

Wêndria C. da Silva, João C. Weyl A. Costa, Karlo Q. da Costa (Universidade Federal do Pará – UFPA, Belém, Brasil), André M. Cavalcante, (Ericsson Telecomunicações Ltda., Indaiatuba, Brazil). E-mails: wendria.silva@tucurui.ufpa.br, jweyl@ufpa.br, karlo@ufpa.br, andre.mendes.cavalcante@ericsson.com.

where $k=2\pi/\lambda_0$ is the phase constant of the medium, $\Delta_{m,n} = |\vec{r}_{ref}| - |\vec{r}_{m,n}|$ is the difference between distances, $|\vec{r}_{ref}|$ the distance from the reference element to the user and $|\vec{r}_{m,n}|$ indicates the distance from an arbitrary array element to the user (Fig. 2).

Simulations were performed using the Method of Moments (MoM), which accurately accounts for mutual coupling among elements and reduces computational cost by discretizing only the conductors [5]-[6]. Additionally, phase matching concepts are applied to optimize beam steering performance. This approach involves precise adjustment of the voltage source phases that feed each individual dipole, enabling controlled manipulation of the radiation direction and resulting pattern. The implementation requires: detailed analysis of phase relationships between array elements and application of appropriate techniques to ensure the desired phase coherence across the entire array.

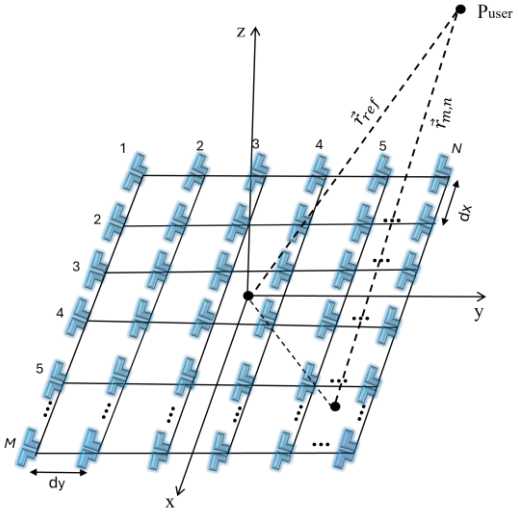

Fig. 2. Geometry of the planar array with *M* by *N* dipoles aligned along x and y axes. The reference vector (r_{ref}) is defined from element *m*=1 and *n*=1 to P_{user}, and $r_{m,n}$ is the general distance vector between element *mn* and P_{user}.

B. Numerical Solution by the Method of Moments

The MoM, also known as the method of mean weighted residuals, is a numerical technique used to solve integral equations in various areas of electromagnetism, covering both the frequency domain and the time domain, including applications in electrostatics, magnetostatics, and electromagnetic scattering. By focusing on electromagnetic sources as the quantities of interest, the MoM becomes highly effective in solving radiation and scattering problems [7]. The method solves complex integral equations by reducing them to a system of simpler algebraic equations, which can be solved numerically using computational tools [8].

The method aims to determine an approximate response function, denoted as *f*, from a linear integro-differential operator *L* and an excitation function *g*, according to the non-homogeneous equation:

$$L(f) = g \tag{2}$$

Function *f* is approximated by a linear combination of N_e terms, with base functions $\hat{f}_p(z')$, which, when inserted in (2), leads to:

$$L(f(z')) \cong \sum_{p=1}^{N_e} I_p L(\hat{f}_p(z')) \cong g \tag{3}$$

From (3), it becomes evident that the unknowns are now the scalar coefficients I_p. If we hypothetically consider the approximate solution, i.e. with N_e basis functions, solving the equation becomes impossible since the number of unknowns N_e exceeds the number of available equations. To determine the scalar quantities I_p, we perform an inner product (integration) with a set of N_e known functions w_q called test or weight functions. These functions must be linearly independent to ensure the N_e equations maintain their independence [8]. Consequently, we obtain a system of linear equations that can be represented in matrix form as $[Z_{qp}][I_p]=[V_q]$ in which $[Z_{qp}]=\langle w_q, L(\hat{f}_p)\rangle$ and $[V_q]=\langle w_q, g\rangle$. The approximate solution can be obtained if the resulting matrix $[Z_{qp}]$ is nonsingular and the scalar coefficients I_p are:

$$[I_p]=[Z_{qp}]^{-1}[V_q] \tag{4}$$

The approximated solution is given by:

$$\hat{f} = \sum_{p=1}^{N_e} I_p \hat{f}_p \tag{5}$$

The solution's convergence depends on the base function $\hat{f}_p$ and test functions, which influence the complexity to determine the matrix elements in the MoM.

III. Numerical Results

Based on the method presented in the previous section, a MoM program was developed in Matlab [9] to calculate the electric field near the arrays. This method approximates the currents from the antenna in a sinusoidal way, disregarding the small transverse variations of the currents in the conductors.

A. Array Design

The antenna elements used in this work are half-wave dipoles at 28 GHz with a length of *l=5mm*. The feeding parameters were defined based in (1), applying a progressive periodic shift to form a array (Fig. 3). The total array size in the *y*-direction is given by $L_y=(N-1)\times dy$ and in the *x*-direction is given by $L_x=(M-1)\times dy$. Fig. 3 shows the two array analyzed, one linear with *M*=1 and *N*=20 and other planar with *M=N*=20, where both arrays have $dy=dx=0.55\lambda_0$. In this case the planar array presents a square shape. To enable near-field beamforming, the feeding phases were further adjusted as (1) to focus the radiation toward a specified user location, denoted as P_{user} (Fig. 2), localized at *x=y*=0 and $z=4L_y$.

Fig. 4 presents the the magnitude of the total electric field distribution near the array planes at *z=0.4 mm*. This results confirm that resonance occurs at half-wavelength along the arms of each dipole in both array types. This is evidenced by

the strong field confinement around the ends of the dipoles in both configurations.

B. Beamforming Array Comparative Analysis

Using the MoM, a comparative analysis was carried out to understand the influence of the size and geometry of the arrangement on the formation of beams in the near-field. Tables I and II present a comparison between linear and planar arrays, considering structural aspects, performance and computational cost of the simulations.

Table I highlights that, although the planar array offers greater directivity and beamforming capacity in two dimensions, it also has greater complexity and computational.

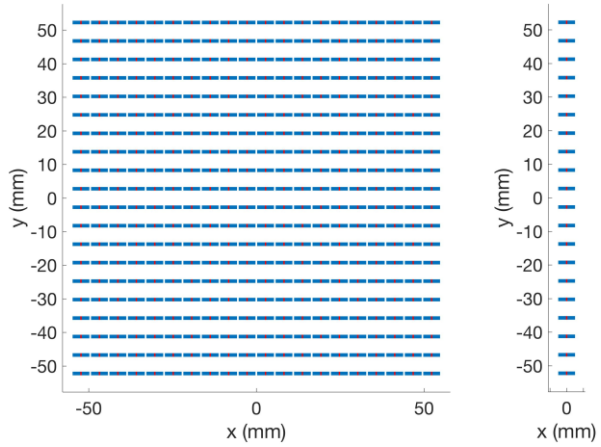

Fig. 3. Geometry of the analyzed arrays generated in Matlab: on the left, planar array 20×20; on the right, linear array 1×20.

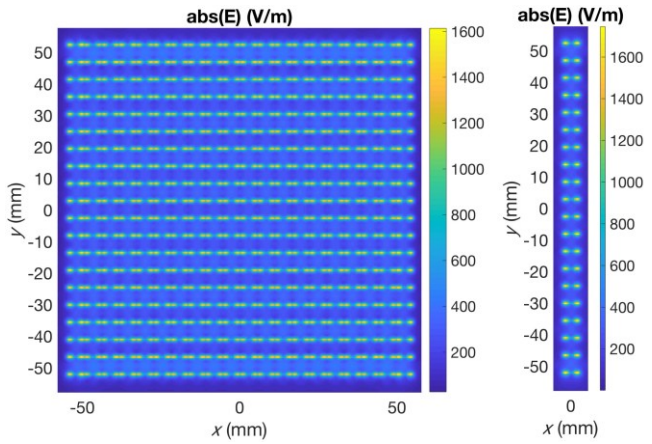

Fig. 4. Distribution of total electric field module abs(E) (V/m) radiated by the arrangement with dy=dx=0.55λ_0 in plane z = 0.4mm: left image for planar array and right image for linear array.

Table II shows that the simulation times for different observation planes increase significantly in the planar case, reaching up to 6 hours (Intel i7, 16G RAM), while the linear array requires considerably less time. These results highlight the trade-off between performance and computational cost in the use of ELAAs for near-field communications [10].

Figs. 5 to 7 illustrate the modulus distributions of the total electric field $|E|$ in (V/m) radiated, in the planes x=0, y=0 and z=4L_y, respectively, for the two dipole arrays: a linear one (on the top or right) and a planar one (on the bottom or left).

It is observed that the planar array provides a significantly more confined beam both in width (y-axis) and depth (z-axis), when compared to the linear arrangement, which exhibits a wider and more diffuse beam. This greater degree of spatial confinement in the planar array produces a better spatial orthogonality of the channels, made possible by the near-field spherical propagation. When in this regime, it becomes possible to distinguish users not only by their angular direction, but also by their radial position (distance), which expands the DoFs available for spatial multiplexing [11].

TABLE I. STRUCTURAL AND SIMULATION COMPARISON OF LINEAR AND PLANAR ARRAYS

Aspect	Linear Array	Planar Array
Dimensionality	*1D (line of dipoles)*	*2D (dipole matrix)*
Number of elements (M × N)	(1 x 20)	(20 x 20)
Directivity	*Moderate*	*High*
Beamforming capability	*One direction*	*Two directions*
Implementation complexity	*Low*	*High*
Computational cost	*Lower*	*Higher*
Simulation time to solve (4)	*3 seconds*	*15 minutes*

TABLE II. SIMULATION TIME TO EVALUATE PLANAR ELECTRIC FIELD DISTRIBUTIONS

Plane	Linear	Planar
x=0 (300*600), 0<z<8Ly ; -2Ly<y<2Ly	*16 min*	*6 h*
y=0 (300*600), 0<z<8Ly ; -2Ly<x<2Ly	*15 min*	*5 h 22 min*
z=0.4mm (300*300), -0.5Ly<x,y<0.5Ly	*8 min*	*4 h 20 min*
z=4Ly (300*300), -0.5Ly<x,y<0.5Ly	*8 min*	*2 h 36 min*

Unlike far-field scenarios, where channel orthogonality between distinct users is primarily achieved in the angular domain and requires large antenna apertures, the near-field regime also exhibits orthogonality in the distance domain. Consequently, users located in the same direction but at different distances can be served simultaneously without interference. This enables *spatial beamforming* (angle plus distance focusing), which reduces inter-user interference and enhances channel capacity [3].

An important aspect observed is that, as the N elements in the array increase (maintaining the relative user position), the region of constructive interference becomes smaller, as can be seen in Figs. 6 and 7, improving the spatial resolution. This is because the phase difference between consecutive dipoles decreases, narrowing the angular width of the beam — behavior analogous to that observed in the far-field [12].

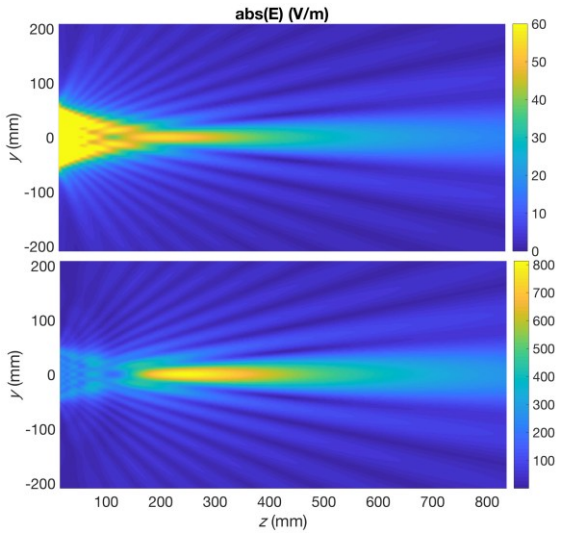

Fig. 5. Distribution of total electric field module abs(E) (V/m) radiated by the arrangement with dy=dx=0.55λ_0 in the plane x=0: upper image is linear array and the lower one being the planar array.

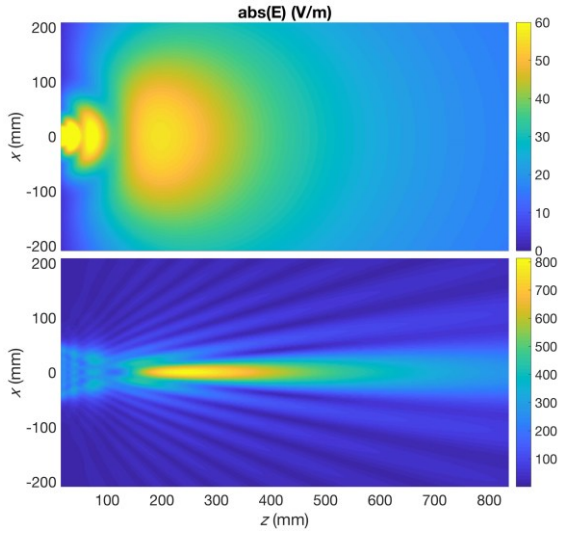

Fig. 6. Distribution of total electric field module abs(E) (V/m) radiated by the arrangement with dy=dx=0.55λ_0 in the plane y=0: upper image is linear array and the lower one being the planar array.

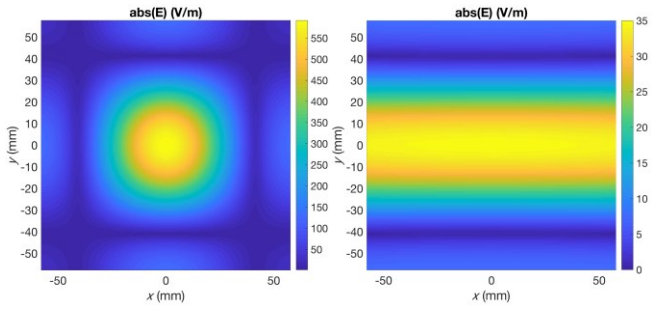

Fig. 7. Distribution of total electric field module abs(E) (V/m) radiated by user height array, plane z=4L_y: left image for planar array and right image for linear array.

However, increasing N reduces inter-element spacing for a fixed aperture, which may introduce mutual coupling and degrade capacity. To suppress grating lobes, arrays are typically designed with a maximum spacing around $\lambda/2$, as determined by Nyquist's spatial criterion. Thus, the core objective of near field communication (NFC) array design is to extend the near-field region relative to the antenna array, enabling more communication users to benefit from near-field beamforming advantages. As evidenced by the Rayleigh distance expression, the matrix aperture is the key to determine the near-field region's extension [13].

Furthermore, at the mmWave and THz frequencies, possible in sixth-generation (6G) communications, propagation is attenuated by molecular absorption, requiring adaptive power allocation. This makes it essential to make efficient use of resources in the near field, whose metrics and constraints differ significantly from those in the far field [14]. Signal quality can degrade faster over long distances at higher frequencies, making adaptive resource management crucial, with higher power allocated to lower frequencies [15].

In summary, NFC resource management differs from its far-field counterpart in several aspects, including available resources and performance metrics, resulting in different optimization objectives and constraints compared to Far-Field Communication (FFC). Simultaneously, the near-field effect presents new challenges, as it often involves large-scale antenna arrays, leading to high-dimensional optimization problems that require intensive use of computation and new mathematical tools [16].

Finally, near-field beamforming also shows promise for physical information security. By focusing energy with high accuracy on the position of the legitimate user, leakage to possible nearby intruders is reduced. As a solution, near-field beamforming can focus the energy of the confidential signal at the target user's location and thus significantly reduce information leakage. This constitutes a promising application of near-field information protection in 6G wireless networks — a scenario where far-field beamforming fails [17].

C. Beamforming Array with Four Users

Using the MoM code, this section presents an example application of the planar array of the previous sections to beamforming multiple users simultaneously. In this case four users are considered with their localizations presented in Table III. In this situation all the users are in the same plane (z=4L_y) that is parallel to the array plane (z=0), where the user 1is centered with the planar array and the other users are shifted from the center by the distance L_y.

TABLE III. RECTANGULAR COORDENATES OF THE USER'S LOCALIZATIONS

User	x	y	z
1	0	0	4L_y
2	L_y	0	4L_y
3	0	L_y	4L_y
4	L_y	L_y	4L_y

Fig. 8 presents the modulus distributions of the total electric field $|E|$ in (V/m) radiated in the parallel plane z=4L_y. This results shows that there are no interferences among the users when the distances among them are L_y at the plane z=4L_y. In this case, the spatial resolution of the beamforming, related to 3dB points, is about 0.5L_y (Fig. 8).

Fig. 9 presents the modulus distributions of the total electric field $|E|$ in (V/m) radiated in the perpendicular planes x=0 (upper image) and x=L_y (lower image). These results show that the spatial resolutions in the perpendicular planes are higher than those of the parallel plane (Fig. 8). Also, the spatial resolution in the radial direction at the plane x=0 is about 4L_y (Fig. 9 upper) and in the plane x=L_y is near L_y (Fig. 9 lower).

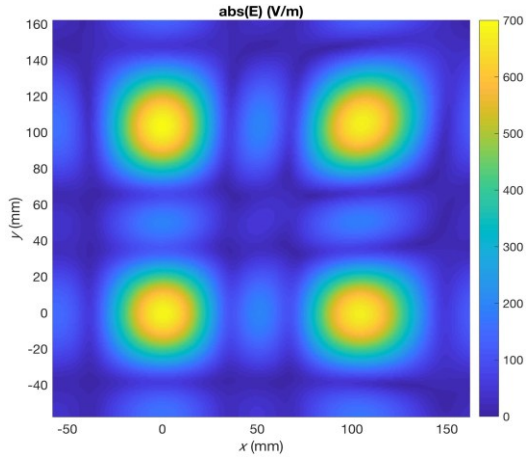

Fig. 8. Distribution of the total electric field module abs(E) (V/m) radiated by the array at the height of the four users in the plane z=4L_y.

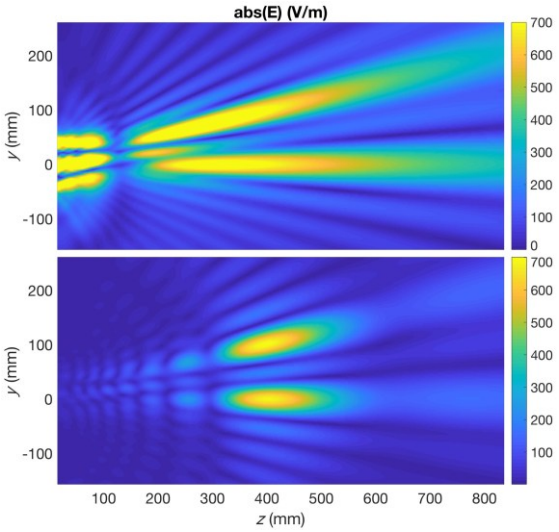

Fig. 9. Distribution of total electric field module abs(E) (V/m) radiated by the array in the planes x=0 (upper image) and x=L_y (lower image).

IV. Conclusions

This study analyzed the radiation behavior of linear and planar dipole arrays in the near field, focusing on beamforming at high frequencies. Using the MoM, it was shown how phase variation between elements enables precise electromagnetic field focusing.

Results revealed that planar arrays with more elements produce narrower beams, improving spatial resolution and allowing higher connection density with reduced interference—key for spatial multiplexing in dense networks. Furthermore, in near-field operation, ELAAs can exploit additional DoFs in both angular and radial domains, enhancing channel capacity.

Finally, the analysis highlights the need to consider mutual coupling in dense arrays and to adapt classical DoF concepts to the near-field regime to ensure optimal system performance, particularly in future 6G applications involving precise beamforming and secure communication.

Acknowledgements

This work was supported by the Innovation Center, Ericsson Telecomunicações Ltda., Brazil and the National Council for Technological and Scientific Development (CNPq).

References

[1] Markit, I. H. S. "The 5G Economy: How 5G will contribute to the global economy." *Qualcomm, Report*, 2019.

[2] Y. Zhao, L. Dai, J. Zhang, "6G near-field technologies white paper." Future Forum, pp. 13-77, 2024.

[3] Liu, Yuanwei, et al. "Near-field communications: A comprehensive survey." *IEEE Communications Surveys & Tutorials*, 2024.

[4] Zhang, Haiyang et al, "6G wireless communications: From far-field beam steering to near-field beam focusing," *IEEE Communications Magazine*, pp 1-3, 2023.

[5] C. A. Balanis, *Antenna Theory: Analysis and Design*, John wiley & sons, 4rd ed, Inc., Hoboken: New Jersey, 2016.

[6] C, K. Queiroz and V. Dmitriev. "Simple and Efficient Computational Method to Analyze Cylindrical Plasmonic Nanoantennas." *International Journal of Antennas and Propagation*, v. 2014, pp. 1-8, 2014.

[7] C. A. Balanis, *Advanced Engineering Electromagnetics*, John Wiley & Sons, 3rd ed, Reino Unido: Wiley, 2024.

[8] D. G. Dudley, *Mathematical Foundations for Electromagnetic Theory*, New York: IEEE Press, 1994.

[9] Matlab software. https://www.mathworks.com/products/matlab.html.

[10] M. M. M. Freitas et al., "Scalable User-Centric Distributed Massive MIMO Systems With Restricted Processing Capacity," *IEEE Transactions on Wireless Communications,* vol. 23, no. 12, pp. 19933–19949, 2024.

[11] Ramezani, Parisa, et al. "Exploiting the depth and angular domains for massive near-field spatial multiplexing." *IEEE BITS the Information Theory Magazine*, v. 3, no. 1, pp 14-26, 2023.

[12] C. Ouyang, Y. Liu, X. Zhang, and L. Hanzo, "Near-field communications: A degree-of-freedom perspective," *arXiv preprint arXiv:2308.00362*, 2023.

[13] H. L. Van Trees, Optimum Array Processing: Part IV of Detection, Estimation, and Modulation theory. John Wiley & Sons, 2002.

[14] C. Han, W. Gao, N. Yang, and J. M. Jornet, "Molecular absorption effect: A double-edged sword of terahertz communications," *IEEE Wireless Communications*, vol. 30, no. 4, pp. 140–146, 2023.

[15] J. An et al., "Near-field communications: Research advances, potential, and challenges," *IEEE Wireless Communications*, vol. 31, no. 3, pp. 100–107, 2024.

[16] Xu, Bokai et al. "Resource allocation for near-field communications: Fundamentals, tools, and outlooks." *IEEE Wireless Communications*, 2024.

[17] Z. Zhang, Y. Liu, Z. Wang, X. Mu, and J. Chen, " "Physical layer security in near-field communications." *IEEE Transactions on Vehicular Technology*, vol. 73, no. 7, pp. 761–10, 2024.